RESEARCH ARTICLE

DOI: 10.4274/tjh.galenos.2025.2024.0365
Turk J Hematol 2025;42:33-46

Identification of TRAPPC4 as a Key Autoantigen in Immune-Related Pancytopenia: Epitope Characterization and Immune Activation Mechanisms

İmmün Aracılı Pansitopenide TRAPPC4'ün Anahtar Otoantijen Olarak Tanımlanması: Epitop Karakterizasyonu ve İmmün Aktivasyon Mekanizmaları

Shanfeng Hao[1,2,3]*, Yang Zhang[1,2,3]*, Na Xiao[1], Zonghong Shao[1,2,3]

[1]*Tianjin Medical University General Hospital, Department of Hematology, Tianjin, China*
[2]*Tianjin Key Laboratory of Bone Marrow Failure and Malignant Hemopoietic Clone Control, Tianjin, China*
[3]*Tianjin Institute of Hematology, Tianjin, China*

These authors contributed equally to this work.

Abstract

Objective: Immune-related pancytopenia (IRP) is characterized by autoantibody-mediated destruction or suppression of bone marrow cells, leading to pancytopenia. This study aimed to explore the role of trafficking protein particle complex subunit 4 (TRAPPC4) as a key autoantigen in IRP, including epitope identification and immune activation mechanisms.

Materials and Methods: A total of 90 participants were included in the study, divided into four groups: 30 newly diagnosed IRP patients, 25 patients with IRP in remission, 20 patients with other hematological conditions (severe aplastic anemia [SAA] and myelodysplastic syndrome [MDS]) as a patient control group, and 15 healthy individuals as a healthy control group. TRAPPC4 was identified using affinity screening with a phage-display random peptide library and confirmed with ELISPOT and epitope prediction software. TRAPPC4 expression in bone marrow cells and serum antibody titers was assessed via flow cytometry, ELISA assay, and real-time polymerase chain reaction. Immune cell profiling of peripheral blood mononuclear cells was conducted using flow cytometry.

Results: TRAPPC4 was overexpressed in the CD34+ bone marrow hematopoietic progenitor cells of newly diagnosed IRP patients compared to patients in remission, the patient control group (SAA and MDS), and the healthy control group, with no significant differences observed for CD15+ granulocytes or CD235a+ nucleated red blood cells. The epitope peptide YTADGKEVLEYLG activated Th2 cells, as confirmed by ELISPOT. Newly diagnosed IRP patients exhibited elevated TRAPPC4 mRNA and protein levels in bone marrow mononuclear cells and higher serum antibody titers compared to controls. Immune

Öz

Amaç: İmmün ilişkili pansitopeni (IRP), kemik iliği hücrelerinin otoantikor aracılı yıkımı veya baskılanması ile karakterize olup pansitopeniye yol açar. Bu çalışma, epitop tanımlama ve immün aktivasyon mekanizmaları da dahil olmak üzere, IRP'de anahtar bir otoantijen olarak 'trafficking protein particle complex subunit 4'ün (TRAPPC4)' rolünü araştırmayı amaçlamıştır.

Gereç ve Yöntemler: Çalışmaya dört gruba ayrılan toplam 90 katılımcı dahil edilmiştir: Yeni tanı konmuş 30 IRP hastası, remisyondaki 25 IRP hastası, hasta kontrol grubu olarak diğer hematolojik durumları olan 20 hasta (ağır aplastik anemi [SAA] ve miyelodisplastik sendrom [MDS]) ve sağlıklı kontrol grubu olarak 15 sağlıklı birey TRAPPC4, bir faj-görüntü rastgele peptid kütüphanesi ile afinite tarama kullanılarak tanımlanmış ve ELISPOT ve epitop tahmin yazılımı ile doğrulanmıştır. Kemik iliği hücrelerindeki TRAPPC4 ifadesi ve serum antikor titreleri akım sitometri, ELISA testi ve gerçek zamanlı polimeraz zincir reaksiyonu ile değerlendirilmiştir. Periferik kan mononükleer hücrelerinin immün hücre profili akım sitometri kullanılarak gerçekleştirilmiştir.

Bulgular: TRAPPC4, yeni tanı konmuş IRP hastalarının CD34+ kemik iliği hematopoetik progenitör hücrelerinde remisyondaki hastalara, hasta kontrol grubuna (SAA ve MDS) ve sağlıklı kontrol grubuna kıyasla aşırı ifade edilirken, CD15+ granülositler veya CD235a+ çekirdekli kırmızı kan hücreleri için anlamlı bir fark gözlenmemiştir. YTADGKEVLEYLG epitop peptidi, ELISPOT ile doğrulandığı üzere Th2 hücrelerini aktive etmiştir. Yeni tanı konulan IRP hastalarında kemik iliği mononükleer hücrelerinde yüksek TRAPPC4 mRNA ve protein seviyeleri ve kontrollere kıyasla daha yüksek serum antikor titreleri görülmüştür. İmmün profilde IRP hastalarında artmış CD19+ ve CD5+CD19+ B lenfositleri gösterilmiştir.

Address for Correspondence/Yazışma Adresi: Zonghong Shao, M.D., Department of Hematology, Tianjin Medical University General Hospital, Department of Hematology; Tianjin Key Laboratory of Bone Marrow Failure and Malignant Hemopoietic Clone Control; Tianjin Institute of Hematology, Tianjin, China.
E-mail: szhong1235@163.com **ORCID:** orcid.org/0000-0003-4966-2956

Received/Geliş tarihi: September 28, 2024
Accepted/Kabul tarihi: January 16, 2025

Abstract

profiling revealed increased CD19+ and CD5+CD19+ B lymphocytes in IRP patients.

Conclusion: TRAPPC4 was found to be a key autoantigen in IRP along with CD34+ cells as primary targets of autoantibody attacks. The identification of TRAPPC4 and its epitope provides insights into IRP pathogenesis and suggests potential diagnostic and therapeutic strategies.

Keywords: TRAPPC4, Cytopenia, Autoantigen, Autoantibody, Immune-related

Öz

Sonuç: TRAPPC4, otoantikor ataklarının birincil hedefi olarak CD34+ hücreleri ile birlikte IRP'de önemli bir otoantijen olarak bulunmuştur. TRAPPC4 ve epitopunun tanımlanması IRP patogenezine ışık tutmakta ve potansiyel tanı ve tedavi stratejileri önermektedir.

Anahtar Sözcükler: TRAPPC4, Sitopeni, Otoantijen, Otoantikor, İmmün ilişkili

Introduction

Autoimmune diseases targeting the bone marrow, such as immune-related pancytopenia (IRP), lead to severe conditions like pancytopenia due to immune-mediated destruction of bone marrow cells. Despite advancements in research, the specific autoantigens involved in IRP remain unidentified, limiting the development of targeted therapies [1,2]. Trafficking protein particle complex subunit 4 (TRAPPC4) has emerged as a potential autoantigen [3]. This protein, part of the TRAPP complex, is critical for intracellular transport within the Golgi apparatus, essential for hematopoietic cell function and bone marrow homeostasis [4]. Dysregulated TRAPPC4 has been linked to cancer, neurodegenerative disorders, and immune dysfunctions [5]. Autoantibodies targeting TRAPPC4 may impair its function, triggering cell dysfunction and destruction via complement activation or macrophage phagocytosis, potentially linked to Th2 cell imbalances [6,7].

Research conducted since 2000 has identified TRAPPC4 as a candidate autoantigen in IRP through studies of patients with unexplained hemocytopenia and positive bone marrow mononuclear cell (BMMNC) Coombs test results [8,9]. The pathogenesis of IRP involves T-lymphocyte dysregulation and increased levels of Th2 cells, Th9 cells, and interleukin (IL)-9, promoting autoantibody production [10,11,12]. TRAPPC4's role in vesicular trafficking, autophagy, and hematopoietic cell signaling, particularly through the ERK-MAPK pathway, highlights its potential involvement in IRP pathogenesis. Autoantibodies against TRAPPC4 may impair hematopoietic progenitor cell function, contributing to disease symptoms and allowing them to serve as diagnostic markers.

This study aimed to investigate TRAPPC4's role in IRP and its correlation with disease severity. Identifying TRAPPC4 as a key autoantigen in IRP could enhance diagnostic precision and enable targeted therapies, improving patient outcomes and reducing the side effects associated with broad immunosuppressive treatments.

Materials and Methods

Patients

IRP is a hematological condition caused by immune-mediated destruction or suppression of bone marrow hematopoietic cells, resulting in cytopenia across one or more blood cell lineages. The diagnosis is based on clinical, laboratory, and immunological findings, including evidence of autoantibodies or immune abnormalities detected through assays. The criteria for IRP diagnosis include the following: 1) hemocytopenia or pancytopenia with normal or elevated reticulocyte/neutrophil percentages; 2) bone marrow showing normal or increased erythroid cells with visible erythroblastic islands; 3) exclusion of other causes of primary/secondary hemocytopenia; and 4) positive BMMNC Coombs test results or autoantibodies on bone marrow hematopoietic cells via flow cytometry (FCM). IRP is differentiated from severe aplastic anemia (SAA) and myelodysplastic syndrome (MDS) by the presence of erythroblastic islands (absent in SAA), the lack of MDS-associated dysplastic changes, and immune markers unique to IRP. Other causes of pancytopenia, including infections, nutritional deficiencies, and drug-induced cytopenia, were excluded in this study based on detailed clinical history, laboratory tests, and bone marrow evaluations to ensure diagnostic specificity.

Participants were divided into four groups, including an untreated IRP group (30 newly diagnosed untreated patients), an IRP remission group (25 patients in remission or with significant improvement), a patient control group (20 patients, including 10 with SAA and 10 with MDS, for comparative analysis), and a healthy control group (15 age- and sex-matched individuals without hematological disorders).

The inclusion of a patient control group helped distinguish IRP-specific immunological features from conditions with overlapping clinical presentations. A total of 90 participants, all inpatients from February 2019 to May 2020, were enrolled, although sample availability affected the assay counts. The study was approved by the Tianjin Medical University General Hospital

Ethics Committee (approval no: 20160301, date: March 3, 2016) and informed consent was obtained from all participants.

Screening of the TRAPPC4 Epitope and Synthesis of the Antigen Peptide

In antibody purification, peripheral blood from 23 IRP patients and 10 healthy controls was processed to extract serum and antibodies via affinity chromatography. In peptide library screening, a phage-display random peptide library was used to identify TRAPPC4 epitopes bound by patient serum antibodies. Patient and control sera were coupled with magnetic beads and incubated with the assistance of the library to isolate specific epitopes. Three rounds of screening with increasingly stringent washes were conducted to ensure specificity. For positive clone identification and sequencing, positive phage clones were identified using an enzyme-linked immunosorbent assay (ELISA) and sequences were determined after further amplification and purification.

Sterile Mononuclear Cell Culture

Peripheral blood mononuclear cells (PBMNCs) were isolated from anticoagulated whole blood, cultured in a serum-supplemented medium, and prepared for downstream applications, including the IL-4 ELISPOT assay.

IL-4 ELISPOT

This assay was used to evaluate IL-4 cytokine production in response to stimulation. Positive and negative control groups were included to establish assay sensitivity and background levels. Samples from the experimental groups were stimulated with specific negative control peptides. After incubation, cytokine spots were visualized and quantified.

Detection of TRAPPC4 mRNA Levels by Fluorescence Quantitative Polymerase Chain Reaction (FQ-PCR)

Total RNA was extracted using the RNAprep Pure Kit (Tiangen Biotech, Beijing, China), which includes DNase treatment to remove genomic DNA and ensure RNA purity. Reverse transcription was carried out with the FastQuant RT Kit (Tiangen Biotech), which uses both oligo(dT) and random primers for efficient cDNA synthesis. FQ-PCR was performed on the iQ5 Real-Time System using SYBR Green dye to detect double-stranded DNA (Bio-Rad, Hercules, CA, USA). Primers for TRAPPC4 and GAPDH were synthesized by GENEWIZ (Suzhou, China). The PCR cycling program involved initial denaturation at 95 °C, followed by 45 cycles of denaturation, annealing, and extension. TRAPPC4 mRNA levels were normalized to GAPDH and calculated using the $2^{-\Delta\Delta Ct}$ method.

Detection of TRAPPC4 Expression in Bone Marrow CD34+/CD235a+/CD15+ Cells by FCM

FCM was used to detect TRAPPC4 expression in CD34+, CD235a+, and CD15+ bone marrow cells. Control tubes (negative and isotype) and experimental tubes were prepared. Cells were stained with antibodies, processed with hemolysin, washed, and analyzed using CytExpert software (Beckman Coulter, Brea, CA, USA). Gating strategies were applied to ensure accurate cell population identification.

Determination of CD5+ B Lymphocyte Ratio

The proportion of CD5+ B lymphocytes in bone marrow CD19+ cells was determined using FCM. Antibody-labeled samples were incubated, treated with lysate, and analyzed for co-expression of CD19 and CD5 markers.

Western Blotting for Detection of TRAPPC4 Protein Levels in BMMNCs

Bone marrow samples were collected with heparin as an anticoagulant and BMMNCs were isolated using density gradient centrifugation. Proteins were extracted by lysing cells with RIPA buffer containing protease inhibitors, and their concentrations were measured using the bicinchoninic acid (BCA) protein assay as a colorimetric method detecting protein concentrations via absorbance at 562 nm. Equal amounts of protein (20-30 µg) were separated by sodium dodecyl-sulfate polyacrylamide gel electrophoresis (SDS-PAGE), transferred to polyvinylidene fluoride membranes, blocked with 5% milk in TBS-T solution, and incubated with primary antibodies against TRAPPC4 and GAPDH (loading control) overnight at 4 °C. After washing, membranes were incubated with HRP-conjugated secondary antibodies and protein detection was performed using the enhanced chemiluminescence method. Signals were visualized with an imaging system and band intensity was analyzed using ImageJ software (National Institutes of Health, Bethesda, MD, USA). TRAPPC4 protein levels were normalized to GAPDH for comparative analysis.

Detection of Serum TRAPPC4 Concentration by ELISA

Serum TRAPPC4 levels were measured for 22 untreated IRP patients, 14 patients with IRP in remission, and 5 healthy controls, with these numbers determined by sample availability. Blood samples of 2 mL each were collected and centrifuged at 3000 rpm for 10 min, and the supernatants were stored at -80 °C for analysis. TRAPPC4 quantification was performed with an ELISA kit using a stepwise procedure that included plate washing, standard/sample addition, incubation, biotin-labeled antibody addition, and further incubation with SABC solution. Following substrate addition and reaction termination, absorbance was measured using a plate reader.

Expression and Purification of Recombinant TRAPPC4 Protein

TRAPPC4 gene amplification was performed with specific primers based on cDNA sequences. PCR products were inserted into the pEASY-E1 vector (TransGen Biotech, Beijing, China) and transformed into *Escherichia coli* Trans1-T1 cells. Positive clones

were confirmed via colony PCR and sequencing. For protein expression, plasmids were transformed into *E. coli* BL21 cells, with induction by isopropyl β-D-1-thiogalactopyranoside (IPTG) at 1 mM. Cells were lysed and proteins were purified using Ni-NTA affinity chromatography. Eluted proteins were analyzed by SDS-PAGE and Coomassie staining for purity and then validated by western blotting. Refolding of purified proteins was performed in a urea gradient buffer at 4 °C for 12 h per gradient step. Final protein concentrations were measured using the BCA assay.

Detection of TRAPPC4 Antibody in Bone Marrow Supernatant by ELISA

Bone marrow supernatants were analyzed using an ELISA protocol. Plates were coated with TRAPPC4 protein (2 μg/mL), incubated at 4 °C overnight, washed with phosphate buffered saline with Tween 20, and blocked with 2% bovine serum albumin. Diluted serum samples (1:100) were added, and these mixtures were incubated at 37 °C for 1.5 h and then evaluated with a secondary antibody (1:2500) and 3,3′,5,5′-tetramethylbenzidine substrate. After stopping the reaction, absorbance was measured. The binding index (BI) was calculated using the following formula: BI = (OD sample - OD blank) / (OD control - OD blank). In this formula, "OD control" represents the absorbance of mixed serum from eight randomly selected samples and "OD blank" corresponds to the absorbance of the blank control well.

Statistical Analysis

Statistical analysis was conducted using IBM SPSS Statistics 24.0 (IBM Corp., Armonk, NY, USA), with normally distributed data expressed as values of mean ± standard deviation. A t-test was used for two-group comparisons with $p<0.05$ considered statistically significant. Graphs and figures were created using GraphPad Prism 8.0 software (GraphPad Software Inc., La Jolla, CA, USA).

Results

Screening of the TRAPPC4 Epitope and Synthesis of the Antigen Peptide

Antibodies were obtained from eluents of 10 normal and 23 IRP-mixed serum samples after protein G purification. Following three rounds of screening, eluting phage titers increased, indicating enrichment. ELISA was used for detection and 10 clones were selected based on recognition by patient antibodies but not by normal antibodies. These clones were sequenced, revealing four peptides: WSLGYTG, TIYTTWQ, WSLGYTR, and YTTTLTY. These peptides contained the YT sequence, with two also containing LG. Alignment with TRAPPC4's amino acid sequence highlighted the YTADGKEVLEYLG peptide, suggesting that it could be an antigenic epitope. Further analysis using the Immune Epitope Database predicted antigenic binding to major histocompatibility complex class II molecules, identifying YTADGKEVLEYLGNP as a positive peptide and LALEVAEKAGTFGPG as a negative peptide.

Verifying the Effect of Antigen Peptides on Th2 Cells Using IL-4 ELISPOT Assay

The positive peptide YTADGKEVLEYLGNP significantly stimulated IL-4 production in newly diagnosed IRP patients, whereas the negative peptide LALEVAEKAGTFGPG did not result in a significant increase in IL-4 production (Figure 1).

Detection of TRAPPC4 Expression in Bone Marrow CD34+/CD235a+/CD15+ Cells by FCM

FCM analysis showed varying TRAPPC4 expression levels across cell types and patient groups, reported as percentages of positive cells. TRAPPC4 expression was significantly higher in CD34+ cells from the untreated IRP group (11.74±2.16%) compared to the group of IRP patients in remission (1.01±1.18%), the patient control group (5.24±3.69%), and the healthy control group (0.63±0.91%) ($p<0.05$). However, no significant differences were observed in TRAPPC4 expression in CD15+ or CD235a+ cells across the groups ($p=0.15$ and $p=0.17$, respectively). Furthermore, no increase in TRAPPC4 positivity was found in CD235a+ nucleated red blood cells ($p=0.23$), suggesting that TRAPPC4 dysregulation may be more relevant to early-stage hematopoietic progenitor cells, such as CD34+ cells, rather than terminally differentiated erythroid cells.

Detection of Serum TRAPPC4 Concentration by ELISA

Serum TRAPPC4 levels were significantly higher in untreated IRP patients (0.87±0.44, n=22) compared to IRP patients in remission (0.51±0.41, n=14) and healthy controls (0.41±0.33,

Figure 1. Results of IL-4 ELISPOT assay analysis. The number of spots in experimental group 2 (peripheral blood mononuclear cells + peptide 2) was significantly higher than that in the negative control well. However, there was no difference in the number of spots in experimental group 1 (peripheral blood mononuclear cells + peptide 1) compared to the negative control well.

n=5) (p<0.05). No significant difference was observed between the IRP patients in remission and healthy controls (p=0.19).

Detection of TRAPPC4 mRNA Expression by FQ-PCR

TRAPPC4 mRNA expression was also significantly elevated in untreated IRP patients (0.79±0.87, n=15) compared to IRP patients in remission (0.42±0.44, n=25) and healthy controls (0.22±0.22, n=17) (p<0.05). Additionally, IRP patients in remission had significantly higher TRAPPC4 mRNA levels than the healthy control group (p<0.05).

Detection of TRAPPC4 Protein in BMMNCs by Western Blotting

Western blot analysis demonstrated that the expression level of TRAPPC4 in untreated IRP patients was significantly higher than that in IRP patients in remission or healthy controls (p<0.05) (Figure 2A).

Detection of B-Cells and CD5+ B-Cells by FCM

The proportion of CD19+ cells in PBMNCs was higher in the untreated IRP group (11.72±7.79%) compared to the group of IRP patients in remission (7.64±5.54%), MDS patients (9.89±6.26%), and SAA patients (10.43±7.48%). A statistically significant difference was found only between the untreated IRP group and the IRP remission group (p=0.0033). Similarly, the proportion of CD5+CD19+/CD19+ cells was higher in the untreated IRP group (2.23±2.39%) than in the other groups, with significant differences observed only between the untreated IRP patients and the IRP patients in remission (p=0.0063). The proportion of CD5+CD19+ in PBMNCs was also higher in the untreated IRP group (0.35±0.48%) compared to the other groups, although a significant difference was only observed between the untreated IRP group and the IRP patients in remission (p=0.0050). No significant differences were found between other groups. Supplementary Figure 1 shows FCM results comparing IRP patients and healthy controls.

Expression and Purification of the TRAPPC4 Protein

The *TRAPPC4* gene was amplified by PCR and inserted into the pEASY-E1 vector. Recombinant plasmids were transformed into *E. coli* BL-21, identified by PCR and sequencing, and induced

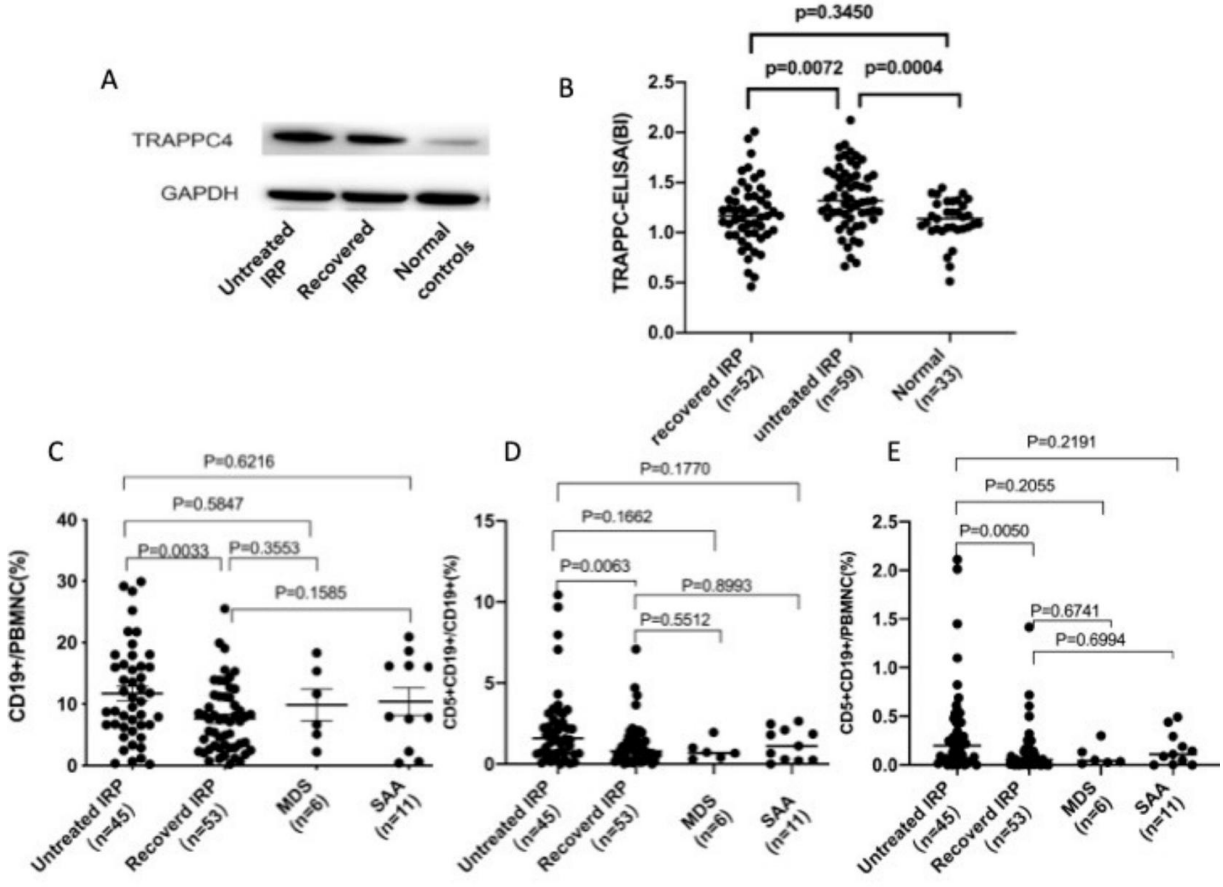

Figure 2. A) TRAPPC4 protein level in bone marrow mononuclear cells detected with Western blotting. B) Anti-TRAPPC4 antibody levels were significantly higher in the serum of untreated immune-related pancytopenia (IRP) patients compared to the IRP patients in remission and healthy controls. C) The proportion of CD19+ in peripheral blood mononuclear cells (PBMNCs) was higher in the untreated IRP group compared to the other groups. D) The proportion of CD5+CD19+/CD19+ cells was higher in the untreated IRP group than in other groups. E) The proportion of CD5+CD19+ in PBMNCs was higher in the untreated IRP group than in other groups.

for expression using IPTG. Fusion proteins were expressed, confirmed by Western blot with an anti-histidine antibody, and purified with ProteinIso Ni-NTA Resin (TransGen Biotech). The optimal imidazole elution concentration for the TRAPPC4 protein was 500 mM. The protein was renatured by dialysis, and its concentration, measured using the BCA method, was 622.5 μg/mL (Figures 3 and 4).

Detection of TRAPPC4 Antibody Levels in the Bone Marrow Supernatant of Patients with IRP by ELISA

The levels of anti-TRAPPC4 antibodies in the serum of untreated IRP patients (1.35±0.31 AU) were higher compared to those of IRP patients in remission (1.18±0.32 AU) and the healthy control group (1.12±0.21 AU), and these differences were statistically significant ($p<0.05$). There was not a significant difference in anti-TRAPPC4 antibody levels between IRP patients in remission and healthy controls ($p>0.05$) (Figure 2B).

Linking TRAPPC4 Expression to IRP Pathogenesis

The elevated TRAPPC4 expression at the mRNA and protein levels in untreated IRP patients and the increased anti-TRAPPC4 antibody production suggest that TRAPPC4 plays a role as an autoantigen in autoimmune responses. TRAPPC4 could contribute to Th2 cell activation and IL-4 production, as evidenced by the ELISPOT assay. These findings highlight TRAPPC4 as a potential key molecular target, providing insights into the autoimmune mechanisms of IRP and warranting further investigation into its role in disease progression.

Discussion

This study identified TRAPPC4 as a potential autoantigen in IRP. Elevated TRAPPC4 expression was observed in bone marrow hematopoietic progenitor cells, serum, and mononuclear cells of IRP patients compared to controls. TRAPPC4-specific antibodies and the YTADGKEVLEYLG peptide epitope were shown to activate

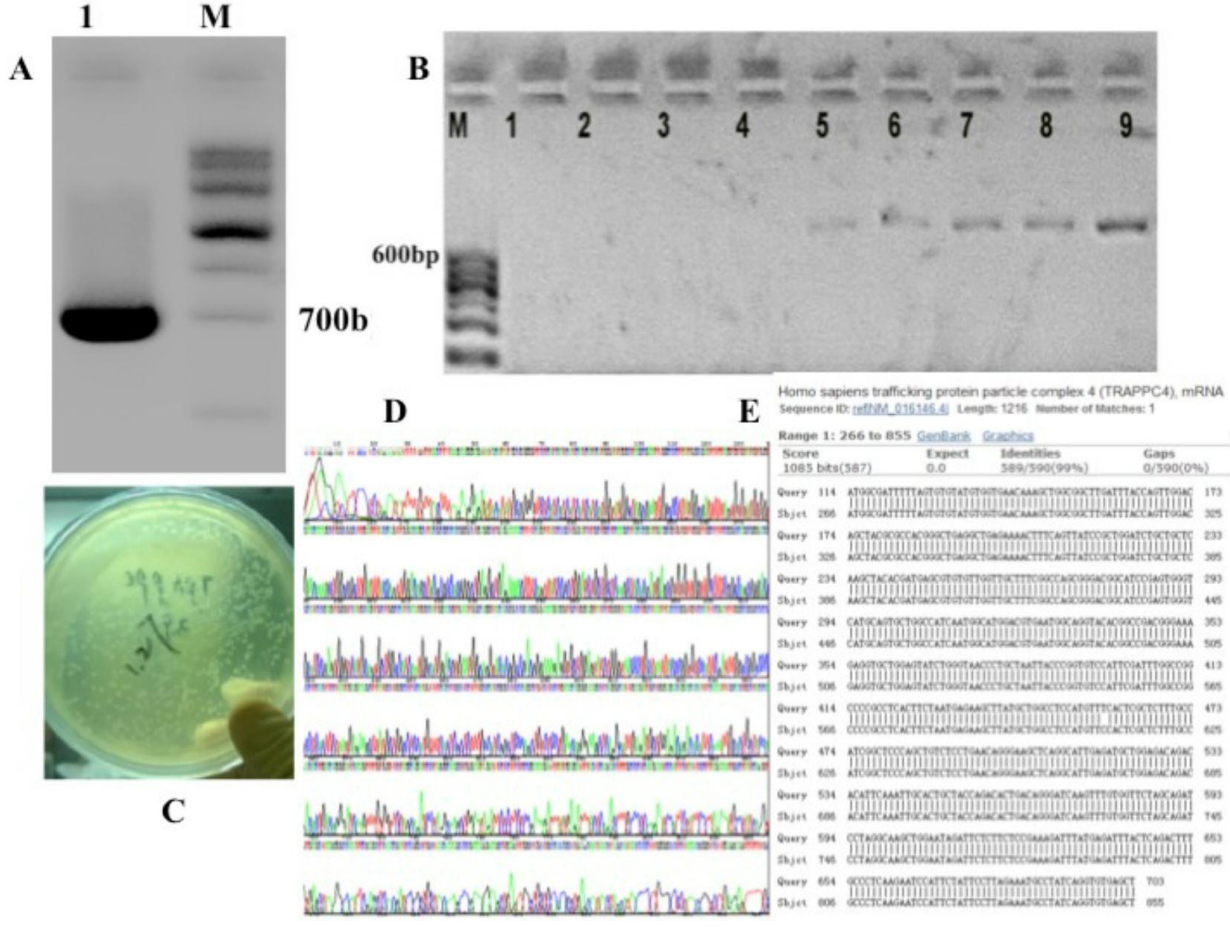

Figure 3. Polymerase chain reaction (PCR) amplification and cloning of TRAPPC4. A) Agarose gel electrophoresis (AGE) result for the open reading frame (ORF) encoding TRAPPC4 amplified from the pTriIEx2-FTL plasmid. Lane markers: M, Tiangen marker I; 1: ORF of TRAPPC4. B) Lanes 1-9 show the AGE results of PCR amplification of eight colonies randomly picked from the plate with vector primer T7-F and primer TRAPPC4-R; lanes 5-9 are forward positive clones. C) Competent *E. coli* Trans1-T1 colonies transformed with the ligated mixture of TRAPPC4 PCR products and expression vector pEASY-E1. D) Sequencing of the plasmid DNA extracted from the forward positive clones with T7 promoter and T7 terminator primer. E) BLAST results showing that the DNA sequences fully coincided with the ORF of TRAPPC4.

Th2 cells, confirming its immunogenicity and involvement in IRP pathogenesis through autoantibody-mediated immune disruption [7,9,13].

IRP, an autoimmune-related form of idiopathic cytopenia of uncertain significance [13,14,15], involves autoantibodies targeting CD34+ hematopoietic progenitor cells. FCM revealed increased TRAPPC4 expression in these cells in newly diagnosed IRP patients compared to patients in remission and the control groups, implicating early hematopoietic cells as primary targets [16,17]. Higher TRAPPC4 mRNA and protein levels in BMMNCs and elevated TRAPPC4-specific antibody titers in the serum of IRP patients further support its pathogenic role. However, no significant increase was noted in CD235a+ nucleated red blood cells, suggesting a focus on early progenitor cells.

TRAPPC4, a core subunit of the TRAPP complex, is critical for intracellular transport, autophagy, and signaling pathways such as ERK-MAPK. Its dysregulation in IRP may impair autophagy, disrupt vesicular trafficking, and promote apoptosis in hematopoietic progenitors. The abnormal membrane localization of TRAPPC4 in IRP patients likely renders it immunogenic, leading to autoimmune responses [5,7,11,16].

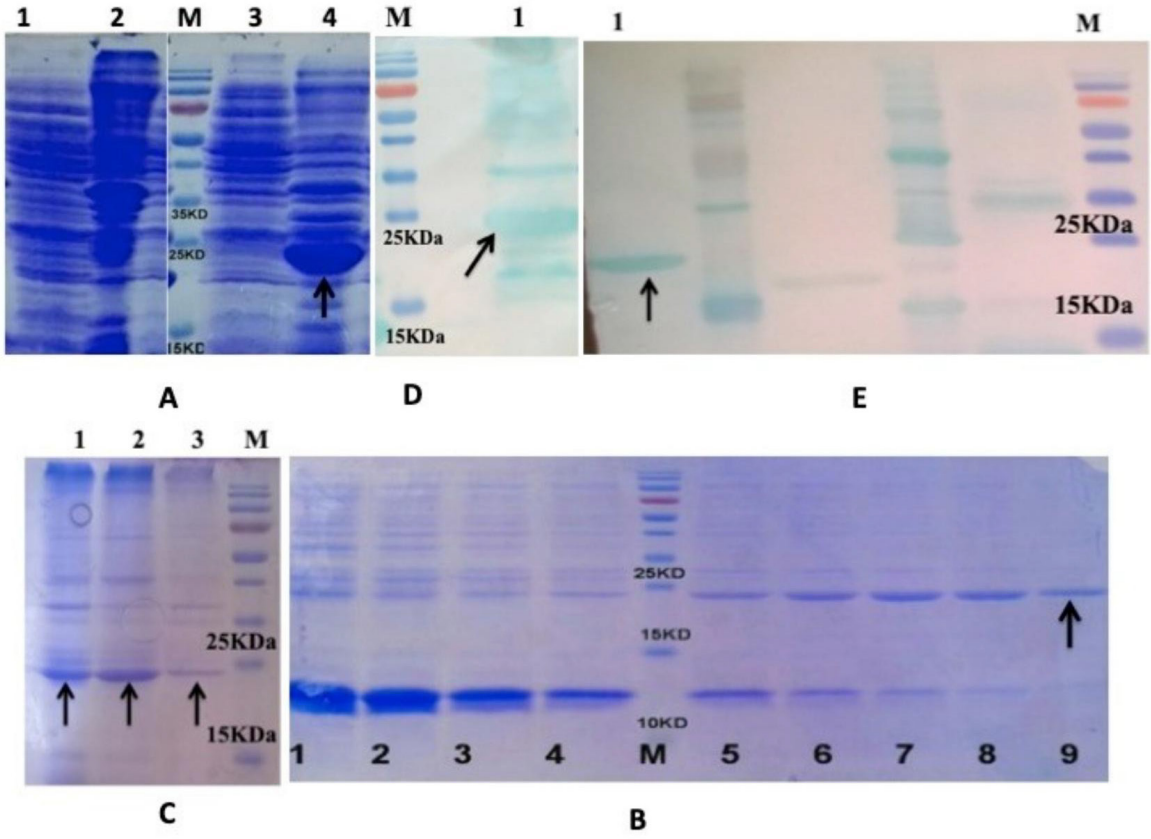

Figure 4. Expression and purification of TRAPPC4. A) Sodium dodecyl-sulfate polyacrylamide gel electrophoresis (SDS-PAGE) analysis of pEASY-E1 in *E. coli* BL21 (DE3) cells and pEASY-E1-TRAPPC4 in *E. coli* BL21 (DE3) cells. Lane M: protein molecular marker; lane 1: supernatant of empty pEASY-E1 in *E. coli* BL21 (DE3) cells; lane 2: precipitation of empty pEASY-E1 in *E. coli* BL21 (DE3) cells; lane 3: supernatant of pEASY-E1-TRAPPC4 in *E. coli* BL21 (DE3) cells; lane 4: precipitation of pEASY-E1-TRAPPC4 in *E. coli* BL21 (DE3) cells. Recombinant TRAPPC4 (rTRAPPC4) was expressed as insoluble protein and accumulated in inclusion bodies. It had a distinct band with molecular weight of about 21.5 kDa (black arrow). B) SDS-PAGE analysis of purified rTRAPPC4 eluted with different concentrations of imidazole. Lane M: protein molecular marker; lanes 1-9: purified rTRAPPC4 eluted with 40, 62.5, 80, 100, 125, 160, 200, 250, and 500 mM imidazole in equilibration buffer (pH 8.0), respectively. Purified rTRAPPC4 eluted with 500 mM imidazole (lane 9, black arrow) had relatively higher purity compared to others and 500 mM was identified as the optimum concentration. (C) SDS-PAGE analysis of purified rTRAPPC4. A total of three purified TRAPPC4 samples were initially loaded (lanes 1-3), and sample 2 was the one that was ultimately selected for subsequent experiments due to its relatively higher purity compared to samples 1 and 3 (black arrow points to the target protein rTRAPPC4). D) Western blotting analysis of recombinant HIS-TRAPPC4 protein before purification (black arrow). E) Western blotting analysis of purified recombinant HIS-TRAPPC4 protein (lane 1, black arrow). The other two proteins loaded in other lanes are not relevant to the present study.

Conclusion

Despite promising findings, this study's limitations include its cross-sectional design, small sample size, and lack of mechanistic validation. Future studies should utilize animal models, proteomic analyses, and single-cell RNA sequencing to explore TRAPPC4 regulation and its role in IRP pathogenesis.

Ethics

Ethics Committee Approval: Tianjin Medical University General Hospital Ethics Committee (approval no: 20160301, March 3, 2016).

Informed Consent: Informed consent was obtained from all participants.

Footnotes

Availability of Data and Materials

The data generated and analyzed in this study are provided in the supplementary figures.

Authorship Contributions

Surgical and Medical Practices: S.H.; Concept: Z.S.; Design: Z.S.; Data Collection or Processing: Y.Z., N.X.; Analysis or Interpretation: Y.Z., N.X.; Literature Search: S.H., Y.Z.; Writing: S.H., Y.Z., N.X., Z.S.

Conflict of Interest: No conflict of interest was declared by the authors.

Financial Disclosure: This research was supported by the National Natural Science Foundation of China (Nos. 81600088 and No. 81770118).

References

1. Park M. Overview of inherited bone marrow failure syndromes. Blood Res. 2022;57(Suppl 1):49-54.
2. Xiao N, Hao S, Zhang Y, Shao Z. Roles of immune responses in the pathogenesis of immunorelated pancytopenia. Scand J Immunol. 2020;92:e12911.
3. Ren Y, Qian Y, Ai L, Xie Y, Gao Y, Zhuang Z, Chen J, Chen YX, Fang JY. TRAPPC4 regulates the intracellular trafficking of PD-L1 and antitumor immunity. Nat Commun. 2021;12:5405.
4. He H, Shao Z, Liu H, Song L, Tian P, Cao Z, Zhang Y, Li K, Zhao M, Shi J, He G, Chu Y, Qian L, Yang T. Immunorelated pancytopenia. Zhonghua Xue Ye Xue Za Zhi. 2021;22:79-82.
5. Uehara J, Yoshino K, Sugiyama E, Ohkuma K, Oaku S, Yamashita C, Hiura A, Fujisawa Y. Immune-related pancytopenia caused by nivolumab and ipilimumab combination therapy for unresectable melanoma of unknown primary. J Dermatol. 2020;47:237-239.
6. Kumar S, Jeong Y, Ashraf MU, Bae YS. Dendritic cell-mediated Th2 immunity and immune disorders. Int J Mol Sci. 2019;20:2159.
7. Shao Q, Wang Y, Liu Z, Liu H, Wang Y, Zhao Y, Li L, Fu R. Th9 cells in peripheral blood increased in patients with immune-related pancytopenia. J Immunol Res. 2020;2020:6503539.
8. Groarke EM, Feng X, Aggarwal N, Manley AL, Wu Z, Gao S, Patel BA, Chen J, Young NS. Efficacy of JAK1/2 inhibition in murine immune bone marrow failure. Blood. 2023;141:72-89.
9. Li W, Wang F, Guo R, Bian Z, Song Y. Targeting macrophages in hematological malignancies: recent advances and future directions. J Hematol Oncol. 2022;15:110.
10. Cedzyński M, Thielens NM, Mollnes TE, Vorup-Jensen T. Editorial: the role of complement in health and disease. Front Immunol. 2019;10:1869.
11. Yu X, Wax J, Riemekasten G, Petersen F. Functional autoantibodies: Definition, mechanisms, origin and contributions to autoimmune and non-autoimmune disorders. Autoimmun Rev. 2023;22:103386.
12. Littleton E, Dreger M, Palace J, Vincent A. Immunocapture and identification of cell membrane protein antigenic targets of serum autoantibodies. Mol Cell Proteomics. 2009;8:1688-1696.
13. Saygin C, Godley LA. Genetics of myelodysplastic syndromes. Cancers (Basel). 2021;13:3380.
14. El Jamal SM, Najfeld V, Coltoff A, Navada S. Myelodysplastic syndromes. In: Salama M, (ed). Atlas of Diagnostic Hematology. Dordrecht, Elsevier, 2020.
15. Shin DY, Park JK, Li CC, Park HS, Moon SY, Kim SM, Im K, Chang YH, Yoon SS, Lee DS. Replicative senescence of hematopoietic cells in patients with idiopathic cytopenia of undetermined significance. Leuk Res. 2019;79:22-26.
16. Goto M, Kuribayashi K, Takahashi Y, Kondoh T, Tanaka M, Kobayashi D, Watanabe N. Identification of autoantibodies expressed in acquired aplastic anaemia. Br J Haematol. 2013;160:359-362.
17. Kelkka T, Tyster M, Lundgren S, Feng X, Kerr C, Hosokawa K, Huuhtanen J, Keränen M, Patel B, Kawakami T, Maeda Y, Nieminen O, Kasanen T, Aronen P, Yadav B, Rajala H, Nakazawa H, Jaatinen T, Hellström-Lindberg E, Ogawa S, Ishida F, Nishikawa H, Nakao S, Maciejewski J, Young NS, Mustjoki S. Anti-COX-2 autoantibody is a novel biomarker of immune aplastic anemia. Leukemia. 2022;36:2317-2327.

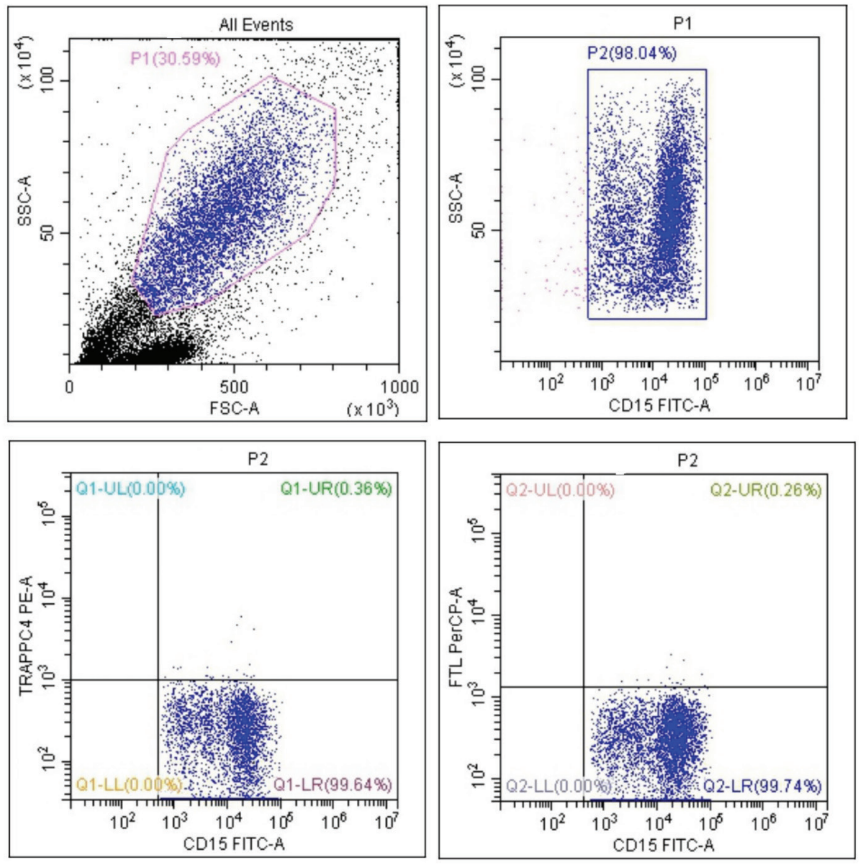

a

Supplementary Figure 1. Flow cytometry results compared between immune-related pancytopenia (IRP) patients and healthy controls.

Figure S1a. CD15 control. Panel A (top left): forward scatter (FSC-A) vs. side scatter (SSC-A) (all events): this scatter plot shows the distribution of all events based on FSC-A and SSC-A, representing cell size and granularity, respectively. The gated population, labeled P1, which accounts for 30.59% of the total events, is shown within magenta contouring. Panel B (top right): CD15 FITC-A vs. SSC-A (P1-gated): after gating on the P1 population, this plot shows CD15 expression (FITC-A) on the x-axis versus SSC-A on the y-axis. A rectangular gate, labeled P2 (98.04%), isolated the population of CD15-positive cells. Panel C (bottom left): CD15 FITC-A vs. TRAPPC4 PE-A (P2-gated): this plot presents CD15 expression (FITC-A) against TRAPPC4 fluorescence (PE-A) for the P2 gated population. Events were sorted into quadrants to identify distinct populations. Q1-LR (99.64%) represents cells that are CD15-positive and TRAPPC4-negative, while Q1-UR (0.36%) corresponds to a small subset of cells co-expressing both markers. Panel D (bottom right): CD15 FITC-A vs. FTL PerCP-A (P2-gated): In this plot, CD15 expression (FITC-A) is shown against FTL fluorescence (PerCP-A) for the P2-gated population. The majority of events fall into Q2-LR (99.74%), which corresponds to cells that are CD15-positive and FTL-negative. A small population (Q2-UR, 0.26%) represents cells that co-express both markers.

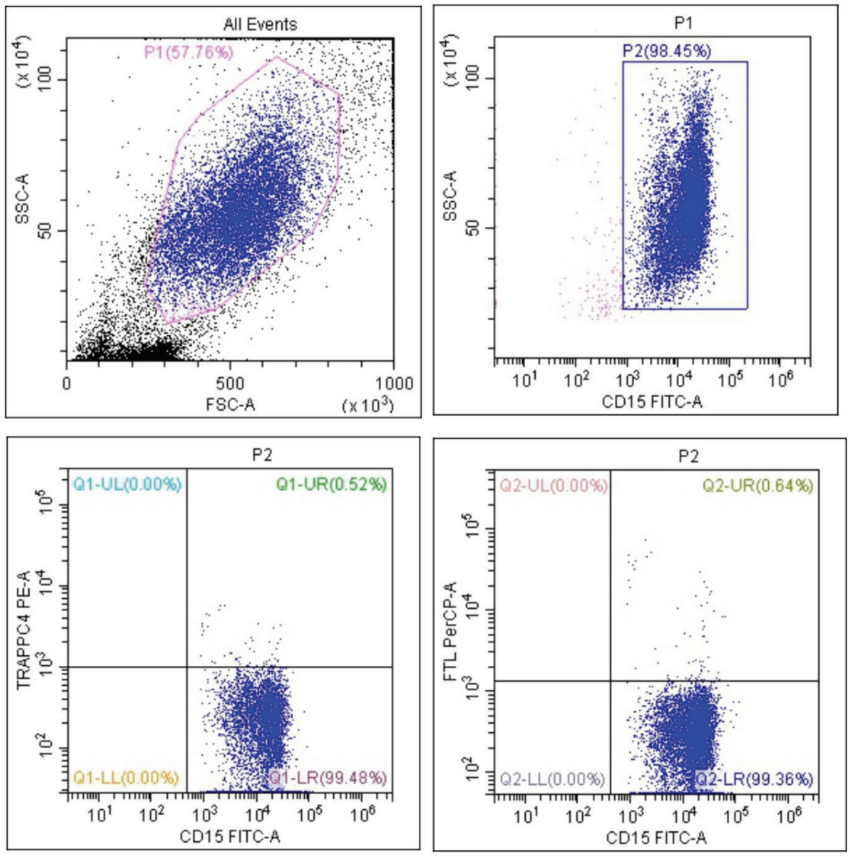

b

Figure S1b. CD15 IRP. Panel A (top left): FSC-A vs. SSC-A (all events): this scatter plot shows the distribution of all events based on FSC-A and SSC-A, indicating cell size and granularity. The gated population, labeled P1, comprises 57.76% of the total events. Panel B (top right): CD15 FITC-A vs. SSC-A (P1-gated): this plot shows CD15 expression (FITC-A) on the x-axis versus SSC-A on the y-axis for the P1-gated population. Gate P2 (98.45%) isolated the CD15-positive population. Panel C (bottom left): CD15 FITC-A vs. TRAPPC4 PE-A (P2-gated): this plot presents CD15 expression (FITC-A) against TRAPPC4 fluorescence (PE-A) for the P2-gated population. Quadrant analysis shows Q1-LR (99.48%) with high CD15 and low TRAPPC4 expression, while Q1-UR (0.52%) is a minor population expressing both markers. Panel D (bottom right): CD15 FITC-A vs. FTL PerCP-A (P2-gated): In this plot, CD15 expression (FITC-A) is shown against FTL fluorescence (PerCP-A) for the P2-gated population. The majority of events fall into Q2-LR (99.36%) with high CD15 and low FTL expression, while Q2-UR (0.64%) represents a small population co-expressing both markers.

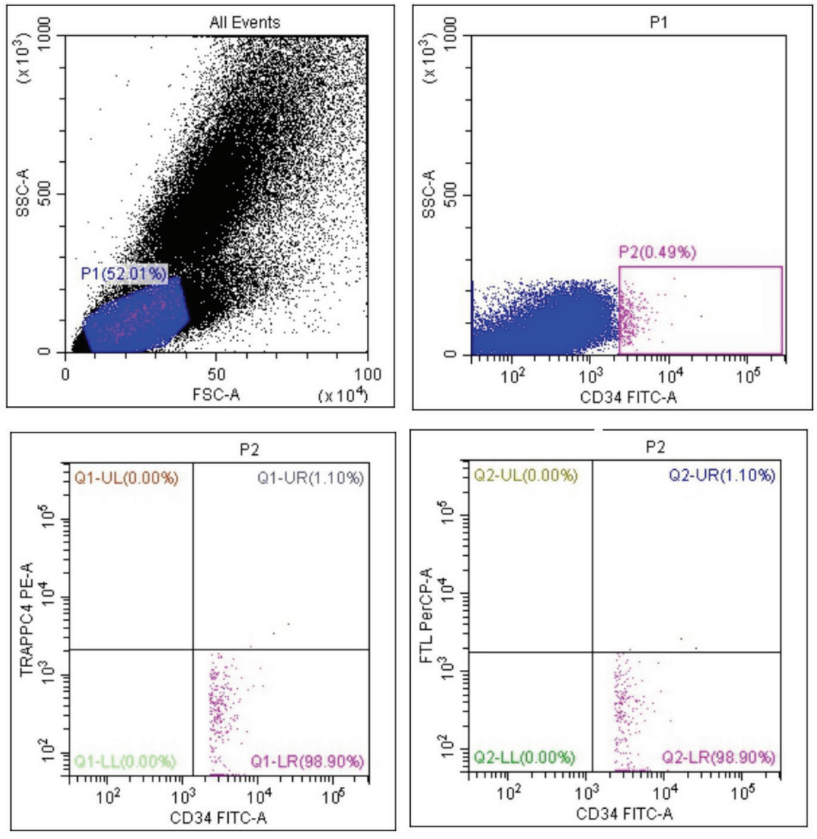

C

Figure S1c. CD34 control. Panel A (top left): FSC-A vs. SSC-A (all events): this scatter plot shows the distribution of all events based on FSC-A and SSC-A, indicating cell size and granularity. Gated population P1 (52.01%) is highlighted by magenta contouring. Panel B (top right): CD34 FITC-A vs. SSC-A (P1-gated): this plot shows CD34 expression (FITC-A) on the x-axis versus SSC-A on the y-axis for the P1-gated population. The P2 gate (0.49%) isolated CD34-positive cells. Panel C (bottom left): CD34 FITC-A vs. TRAPPC4 PE-A (P2-gated): this plot presents CD34 expression (FITC-A) on the x-axis and TRAPPC4 fluorescence (PE-A) on the y-axis for the P2-gated population. Quadrant analysis shows that Q1-LR (98.90%) represents cells that are CD34-positive and TRAPPC4-negative, while Q1-UR (1.10%) represents a small co-expressing population. Panel D (bottom right): CD34 FITC-A vs. FTL PerCP-A (P2-gated): This plot shows CD34 expression (FITC-A) against FTL fluorescence (PerCP-A) for the P2-gated population. The majority of events fall into Q2-LR (98.90%) with high CD34 and low FTL expression, and Q2-UR (1.10%) indicates a minor population co-expressing both markers.

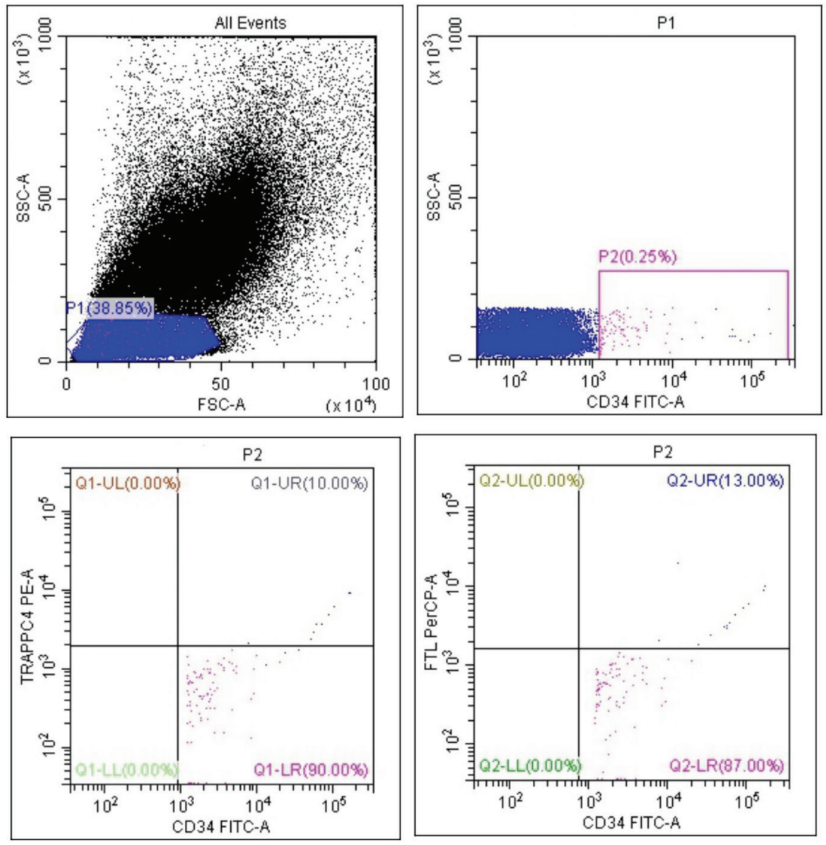

d

Figure S1d. CD34 IRP. Panel A (top left): FSC-A vs. SSC-A (all events): this scatter plot shows the distribution of all events based on FSC-A and SSC-A, indicating cell size and granularity. The gated population, labeled P1, accounts for 38.85% of the total events. Panel B (top right): CD34 FITC-A vs. SSC-A (P1-gated): this plot shows CD34 expression (FITC-A) on the x-axis versus SSC-A on the y-axis for the P1-gated population. Gate P2 (0.25%) isolated the CD34-positive population. Panel C (bottom left): CD34 FITC-A vs. TRAPPC4 PE-A (P2-gated): this plot presents CD34 expression (FITC-A) against TRAPPC4 fluorescence (PE-A) for the P2-gated population. Quadrant analysis shows Q1-LR (90.00%) with high CD34 and low TRAPPC4 expression, and Q1-UR (10.00%) presents a minor population expressing both markers. Panel D (bottom right): CD34 FITC-A vs. FTL PerCP-A (P2-gated): in this plot, CD34 expression (FITC-A) is shown against FTL fluorescence (PerCP-A) for the P2 gated population. The majority of events fall into Q2-LR (87.00%) with high CD34 and low FTL expression, while Q2-UR (13.00%) represents a small population co-expressing both markers.

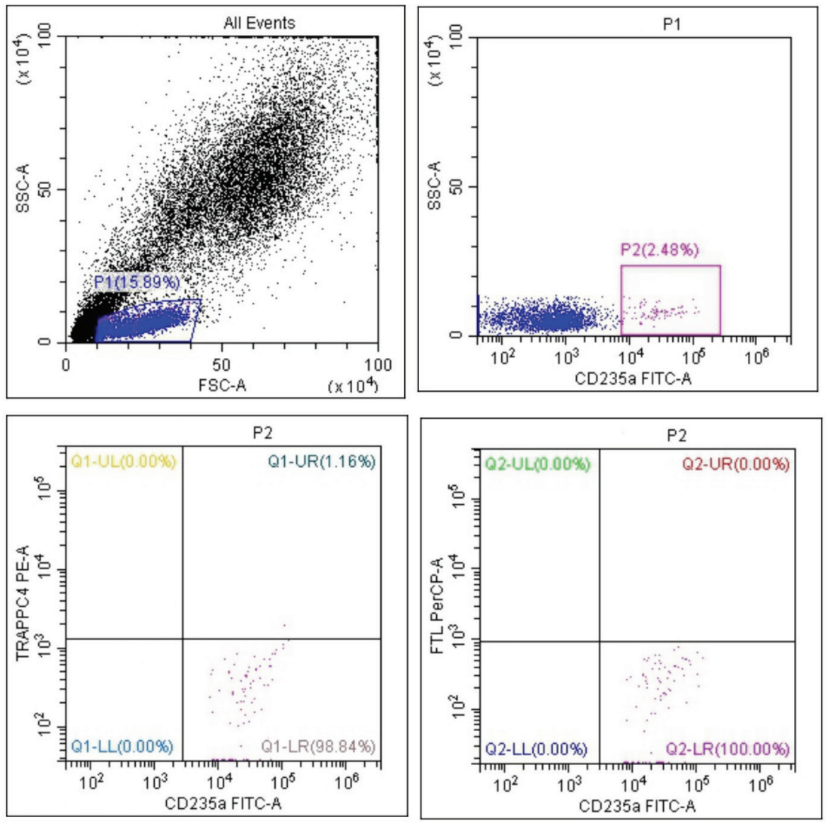

e

Figure S1e. CD235 control. Panel A (top left): FSC-A vs. SSC-A (all events): this scatter plot shows the distribution of all events based on FSC-A and SSC-A, which represent cell size and granularity, respectively. The gated population, labeled P1, which accounts for 15.89% of the total events, is shown within magenta contouring. Panel B (top right): CD235 FITC-A vs. SSC-A (P1-gated): after gating on the P1 population, this plot shows CD235 expression (FITC-A) on the x-axis versus SSC-A on the y-axis. A rectangular gate, labeled P2 (2.48%), isolated the population of CD235-positive cells. Panel C (bottom left): CD235 FITC-A vs. TRAPPC4 PE-A (P2-gated): This plot presents CD235 expression (FITC-A) against TRAPPC4 fluorescence (PE-A) for the P2 gated population. Events were sorted into quadrants to identify distinct populations. Q1-LR (98.84%) represents cells that are CD235-positive and TRAPPC4-negative, while Q1-UR (1.16%) corresponds to a small subset of cells co-expressing both markers. Panel D (bottom right): CD235 FITC-A vs. FTL PerCP-A (P2-gated): In this plot, CD235 expression (FITC-A) is shown against FTL fluorescence (PerCP-A) for the P2-gated population. The majority of events fall into Q2-LR (100.00%), which corresponds to cells that are CD235-positive and FTL-negative. A small population (Q2-UR, 0.00%) consists of cells that co-express both markers.

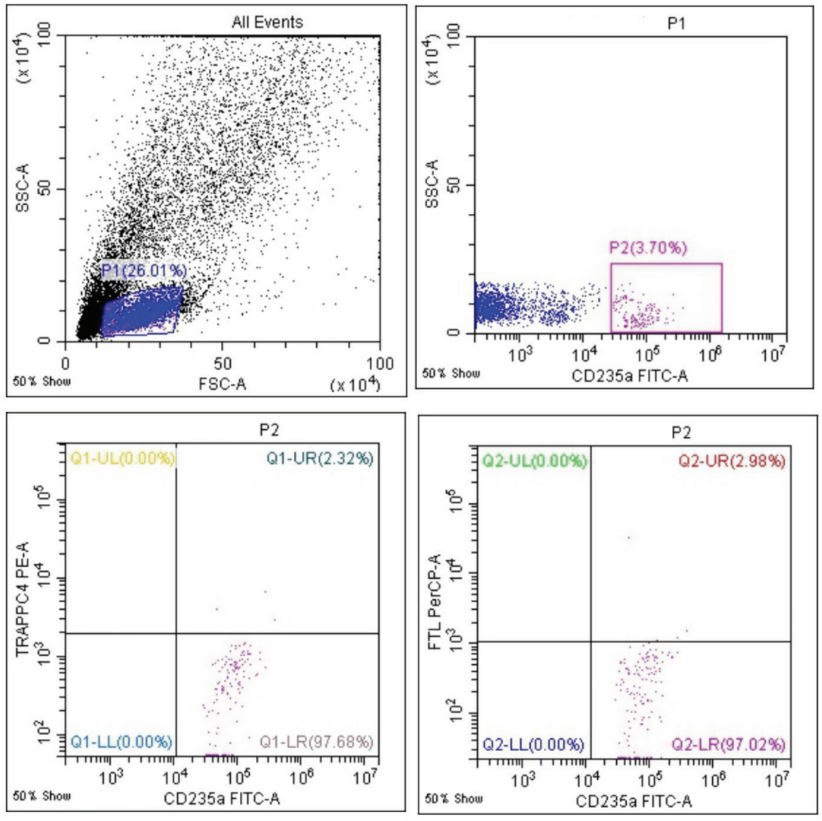

f

Figure S1f. CD235 IRP. Panel A (top left): FSC-A vs. SSC-A (all events): this scatter plot shows the distribution of all events based on FSC-A and SSC-A, indicating cell size and granularity. The gated population, labeled P1, comprises 26.01% of the total events. Panel B (top right): CD235 FITC-A vs. SSC-A (P1-gated): this plot shows CD235 expression (FITC-A) on the x-axis versus SSC-A on the y-axis for the P1 gated population. Gate P2 (3.70%) isolated the CD235-positive population. Panel C (bottom left): CD235 FITC-A vs. TRAPPC4 PE-A (P2-gated): this plot presents CD235 expression (FITC-A) against TRAPPC4 fluorescence (PE-A) for the P2-gated population. Quadrant analysis shows Q1-LR (97.68%) with high CD235 and low TRAPPC4 expression, and Q1-UR (2.32%) is a minor population expressing both markers. Panel D (bottom right): CD235 FITC-A vs. FTL PerCP-A (P2-gated): in this plot, CD235 expression (FITC-A) is shown against FTL fluorescence (PerCP-A) for the P2-gated population. The majority of events fall into Q2-LR (97.02%) with high CD235 and low FTL expression, while Q2-UR (2.98%) represents a small population co-expressing both markers.